ISSN 1070-3284, Russian Journal of Coordination Chemistry, 2013, Vol. 39, No. 8, pp. 571–578. © Pleiades Publishing, Ltd., 2013.

Dipyridyl-Type Ligand-Directed Assembly of Three Cobalt(II) Coordinated Polymers Based on Carboxyphenylpropionate[1]

L. Y. Xin, G. Z. Liu*, X. L. Li, and H. Guo

College of Chemistry and Chemical Engineering, Luoyang Normal University, Henan, Luoyang, 471022 P.R. China

**e-mail: gzliu@yahoo.com.cn*

Received December 7, 2011

Abstract—A series of Co(II)–H_2Cpp coordination polymers incorporating different auxiliary ligands, [Co(Cpp)(Phen)(H_2O)] (**I**), {[Co(Bipy)($H_2O)_4$](Cpp)}$_n$ (**II**), and [Co(Cpp)(Bds)(H_2O)]$_n$ (**III**) (H_2Cpp = 3-(4-carboxyphenyl)propionic acid, Phen = 1,10-phenanthroline, Bipy = 4,4'-bipyridyl, and Bds = 4,4'-bipyridyl sulfide), were synthesized by the hydrothermal reaction and characterized by single crystal X-ray diffraction, elemental analysis, IR, and TG. Three complexes display from 0D to 1D different structural features under the regulation of distinguishing dipyridyl-type coligands. Complex **I** possesses a binuclear Co(II) motif constructed by H_2Cpp and Phen, which further developing a zipper-like 2D layer via H-bonded and π–π stacking interactions. Complex **II** displays straight Bipy-bridging 1D chain, and further forming a 3D supramolecular structure by hydrogen-bonded interactions. Complex **III** exhibits 1D double-chain collectively jointed by Cpp and Bds, which further interlinked into a 3D supramolecular architecture by H-bonded interactions.

DOI: 10.1134/S1070328413070117

INTRODUCTION

The rational design and preparation of metal-organic coordination polymers are greatly important of developing new crystalline materials for their promising applications of catalysis, gas sorption, magnetic, photoluminescent properties and so on [1–5]. The effective and facile approach for the synthesis of such complexes is still the appropriate choice of well-designed organic ligands as bridges or terminal groups (building blocks) with metal ions or clusters as nodes.

Among the reported studies, organic ligands with multi-carboxylate group are particularly interesting for this purpose because they not only possess more than one donor atom to form an extended structure [6–10], but can also act as both hydrogen-bond acceptors and hydrogen-bond donors. Among them a remarkable multidentate carboxylic ligand, 3-(4-carboxyphenyl)propionic acid (H_2Cpp), captures our attention: these ligands combined with rigid –COOH and flexible –CH_2CH_2COOH carboxylate groups can probably produce new structure due to their different coordination modes and molecular flexibility [11–13]. Unfortunately, the semirigid organic linkers are under developed in metal-organic frameworks (MOFs) chemistry, though initial inference on the existence of a number of new structures seems reasonable.

Furthermore, inclusion of neutral dipyridyl coligands in the coordination polymer framework can force adjustment of the carboxylate bridging mode, which can result in significant differences [14, 15]. As a result, the insertion of additional ligands in the synthesis media can have a crucial effect on the dimensionality of the resulting network. These effects are not only due to the coordination mode of the additional ligand (i.e., by blocking positions in the coordination sphere), but also to induce supramolecular interactions, such as π–π stacking interactions, when using aromatic additional depending on the chosen additional nitrogen ligands: chelating and non-chelating pyridines with rigid or flexible structures.

In this contribution we present the extension of our previous work [16, 17] on Zn with H_2Cpp to three new derivatives on the control of three type of additional nitrogen ligands with the range of structural dimensionalities from 0D Co(II) binuclear structure, [Co(Cpp)(Phen)(H_2O)] **(I)**, 1D straight-chain constructed by linear Bipy molecule, {[Co(Bipy)($H_2O)_4$](Cpp)}$_n$ **(II)** to 1D double-stranded chain containing Cpp anion and kinked Bds coligand, [Co(Cpp)(Bds)(H_2O)]$_n$ **(III)**, where Phen = 1,10-phenanthroline, Bipy = 4,4'-bipyridyl, and Bds = 4,4'-bipyridyl sulfide. Three type of ancillary ligands and coordination mode of H_2Cpp observed in complexes **I** and **III** are given in Scheme:

---

[1] The article is published in the original.

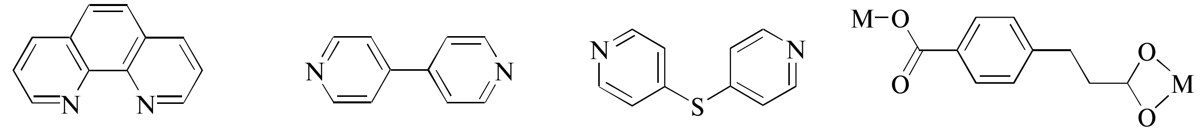

Chelate ancillary ligand (1) Rigid-rod ancillary ligand (2) Kinked ancillary ligand (3) Coordination mode of H_2Cpp (4)

Scheme.

Furthermore, thermal stability of complex **I**–**III** are also given.

EXPERIMENTAL

Materials and physical measurements. All reagents used in the syntheses were of analytical grade. Elemental analyses for C, H, and N atoms were performed on a Vario EL III elemental analyzer. The infrared spectra (4000–600 cm^{-1}) were recorded by using KBr pellet on an Avatar 360 E.S.P. IR spectrometer. The thermogravimetric analyses (TGA) were carried out on a STA449C integration thermal analyzer in flowing N_2 with a heating rate of 10°C/min.

Synthesis of I was carried out by the mixture of $Co(OAc)_2 \cdot 4H_2O$ (0.0249 g, 0.10 mmol), H_2Cpp (0.0194 g, 0.10 mmol), Phen (0.0396 g, 0.20 mmol), NaOH (0.004 g, 0.10 mmol), and 8 mL of water, which were placed in a 23 mL Teflon liner stainless steel reactor. The vessel was heated to 120°C for 4 days, then cooled at 5°C h^{-1} to room temperature. Pink crystals were obtained and filtered off, washed with mother liquid, and dried under ambient conditions. The yield was 50% (based on H_2Cpp ligand).

For $C_{22}H_{18}N_2O_5Co$
anal. calcd., %: C, 58.81; H, 4.04; N, 6.23.
Found, %: C, 58.78; H, 4.16; N, 6.30.

Synthesis of II was carried out by a similar way as that described for **I**, except that Phen was replaced by Bipy. The yield was 43% (based on H_2Cpp ligand).

For $C_{20}H_{24}N_2O_8Co$
anal. calcd., %: C, 50.11; H, 5.05; N, 5.84.
Found, %: C, 50.20; H, 5.21; N, 5.68.

Synthesis of III was also carried out by in a similar way as that described for **I**, except that Phen was replaced by Bds. The yield was 56% (based on H_2Cpp ligand).

For $C_{20}H_{18}N_2O_5SCo$
anal. calcd., %: C, 52.52; H, 3.97; N, 6.12.
Found, %: C, 52.45; H, 4.21; N, 6.05.

X-ray structure determination. The crystallographic data collections for complexes **I**–**III** were carried out a Bruker SMART APEX II CCD diffractometer equipped with graphite-monochromated MoK_α radiation ($\lambda = 0.71073$ Å) by using the φ/ω scan technique at room temperature. Absorption corrections were based on symmetry equivalent reflections using the SADABS program [18, 19]. The structures were solved by direct methods followed by successive difference Fourier syntheses, and a full-matrix least-squares refinement on F^2 was carried out using the SHELX-97 program package with anisotropic thermal parameters for all non-hydrogen atoms. The hydrogen atoms were placed in calculated positions and refined isotropically with a riding model except for those bound to water molecules, which were initially located in a difference Fourier map and included in the final refinement by use of geometrical restraints with the O–H distances being fixed at 0.85 Å and U_{iso}(H) equivalent to 1.5 times of U_{eq}(O). Crystal data and experimental details for compounds **I**–**III** are contained in Table 1. Selected bond distances and angles are listed in Tables 2 and 3, respectively.

Supplementary materials for three compounds have been deposited with Cambridge Crystallographic Data Centre (nos. 855849–855851 for compound **I**–**III**; deposit@ccdc.cam.ac.uk or http://www.ccdc.cam.ac.uk).

RESULTS AND DISCUSSION

Complex **I** displays a 0D Co(II) binuclear structure built the Cpp anion and chelate Phen molecule, and further forming 2D supermolecule network by the H-bonded and π–π stacking interactions. The asymmetric unit of **I** contains one Co^{2+} cation, one Cpp anion, one Phen molecule, and one coordinated water molecule (Fig. 1a). Each Co atom is octahedrally coordinated by three carboxylate O donors of two symmetry-related Cpp anions, one coordinated water molecule, and two N donors of Phen co-ligand adopted a didentaltly chelating mode. Among them, the Co–O bond lengths are in the range of 2.0495(14)–2.1613(15) Å and the Co–N bond lengths are 2.1056(17) and 2.1696(17) Å, respectively.

Both carboxylic groups of the H_2Cpp ligand bridge the Co(II) centers by a monodentatly bridging and a didentaltly chelating mode, respectively (Scheme),

Table 1. Crystal data and structure refinement parameters for **I–III**

Parameter	Value		
	I	**II**	**III**
Formula weight	449.31	479.34	457.35
Temperature, K	296(2)	296(2)	296(2)
Crystal system	Monoclinic	Monoclinic	Monoclinic
Space group	$P2_1/c$	$P2_1/c$	$C2/c$
a, Å	12.6374(13)	12.2246(10)	38.506(10)
b, Å	15.9864(16)	13.3503(11)	8.683(2)
c, Å	10.4090(11)	14.2663(12)	11.721(3)
β, deg	112.0130	113.7980(10)	94.375(3)
Volume, $Å^3$	1949.6(3)	2130.3(3)	3907.5(17)
Crystal size, mm	0.38 × 0.17 × 0.15	0.40 × 0.25 × 0.13	0.42 × 0.18 × 0.10
Z	4	4	8
ρ_{calcd}, g cm^{-3}	1.531	1.495	1.555
μ, mm^{-1}	0.918	0.855	1.021
$F(000)$	924	996	1880
θ Range, deg	2.47–25.50	2.38–25.49	2.40–25.50
Reflections collected	14643	15935	14468
Independent reflections (R_{int})	3622 (0.0278)	3960 (0.0216)	3637 (0.0267)
Parameters	273	280	264
Goodness-of-fit	1.022	1.052	1.036
Final R indices ($I > 2\sigma(I)$)	$R_1 = 0.0299$, $wR_2 = 0.0678$	$R_1 = 0.0314$, $wR_2 = 0.0787$	$R_1 = 0.0307$, $wR_2 = 0.0802$
R indices (all data)	$R_1 = 0.0416$, $wR_2 = 0.0735$	$R_1 = 0.0373$, $wR_2 = 0.0821$	$R_1 = 0.0386$, $wR_2 = 0.0847$
Largest diff. peak and hole, e $Å^{-3}$	0.255 and –0.289	0.768 and –0.601	0.241 and –0.531

forming Co carboxylate dimer (Fig. 1a). Notably, the presence of coordinated water molecule leads to the formation of extensive H-bonding interactions (Fig. 1b). Besides intramolecular O(5*w*)–H(1*w*)···O(3) hydrogen bonds, intermolecular O(5*w*)–H(2*w*)···O(1) interactions further extend the adjacent dimers to produce a 1D double chain along the crystallographic *x* axis (Fig. 1b). The details of the hydrogen bonds are shown in Table 3. Strong π–π stacking interactions (the face to face distance is 3.86 Å) existing between both aromatic rings of Phen coligands from two adjacent 1D chains, result in a zipper-like 2D layer (Fig. 1b). The adjacent 2D layers stack in a slightly off-set parallel fashion with the weak effect of van der Waals force.

Complex **II** exhibits a 1D straight-chain architecture constructed by linear Bipy molecule, and further forming the 3D supermolecule structure by H-bonded interactions. The asymmetric unit contains one Co^{2+} ion, one Bipy molecule, four coordinated water molecule, and uncoordinated Cpp anion. As shown in Fig. 2a, the Co^{2+} ion is located in a six-coordinated slightly distorted octahedron geometry with four symmetry-related water molecules in the equatorial plane (the Co–O bond lengths are in the range of 2.0845(16)–

Table 2. Selected bonds (Å) for compounds **I–III***

Bond	d, Å	Bond	d, Å
I			
Co(1)–O(4)	2.0495(14)	Co(1)–O(1)$^{\#1}$	2.1586(15)
Co(1)–O(5*w*)	2.0872(15)	Co(1)–O(2)$^{\#1}$	2.1613(15)
Co(1)–N(1)	2.1056(17)	Co(1)–N(2)	2.1696(17)
II			
Co(1)–O(3)	2.0845(16)	Co(1)–O(4)	2.0904(16)
Co(1)–O(1)	2.0997(14)	Co(1)–O(2)	2.1007(16)
Co(1)–N(2)$^{\#1}$	2.1640(17)	Co(1)–N(1)	2.1640(17)
III			
Co(1)–O(1)	2.0718(14)	Co(1)–O(5)	2.1114(14)
Co(1)–N(1)	2.1715(18)	Co(2)–O(3)	2.1011(17)
Co(2)–N(2)$^{\#1}$	2.127(2)	Co(2)–O(4)	2.1581(19)

* Symmetry codes for compounds: (**I**) $^{\#1}$ $-x, -y + 1, -z + 1$; (**II**) $^{\#1}$ $x + 1, -y + 1/2, z + 1/2$; (**III**) $^{\#1}$ $-x + 1/2, -y + 1/2, -z$.

Table 3. Selected angles (deg) for compounds **I–III***

Angle	ω, deg	Angle	ω, deg
		I	
O(4)Co(1)O(5*w*)	89.31(6)	O(4)Co(1)N(1)	95.53(7)
O(5*w*) Co(1)N(1)	99.91(6)	O(4)Co(1)O(1)$^{\#1}$	95.75(6)
O(5*w*)Co(1)O(1)$^{\#1}$	101.09(6)	N(1)Co(1)O(1)$^{\#1}$	156.22(6)
O(4)Co(1)O(2)$^{\#1}$	91.23(6)	O(5*w*)Co(1)O(2)$^{\#1}$	161.74(6)
N(1)Co(1)O(2)$^{\#1}$	98.21(6)	O(5*w*)Co(1)N(2)	60.69(6)
O(4)Co(1)N(2)	172.44(7)	O(5*w*)Co(1)N(2)	89.66(6)
N(1)Co(1)N(2)	77.28(7)	O(1)$^{\#1}$Co(1)N(2)	91.79(6)
O(2)$^{\#1}$Co(1)N(2)	92.09(6)		
		II	
O(3)Co(1)O(4)	90.77(7)	O(3)Co(1)O(1)	175.22(6)
O(4)Co(1)O(1)	85.07(6)	O(3)Co(1)O(2)	96.54(7)
O(4)Co(1)O(2)	172.65(6)	O(1)Co(1)O(2)	87.59(6)
O(3)Co(1)N(2)$^{\#1}$	87.56(7)	O(4)Co(1)N(2)$^{\#1}$	90.83(6)
O(1)Co(1)N(2)$^{\#1}$	94.86(6)	O(2)Co(1)N(2)$^{\#1}$	90.24(6)
O(3)Co(1)N(1)	88.13(7)	O(4)Co(1)N(1)	91.89(6)
O(1)Co(1)N(1)	89.64(6)	O(2)Co(1)N(1)	87.61(6)
N(2)$^{\#1}$Co(1)N(1)	174.93(7)		
		III	
O(1)$^{\#1}$Co(1)O(1)	180.00(8)	O(1)$^{\#1}$Co(1)O(5)$^{\#1}$	87.37(6)
O(1)Co(1)O(5)$^{\#1}$	92.63(6)	O(5)$^{\#1}$Co(1)O(5)	180.00(11)
O(1)$^{\#1}$Co(1)N(1)$^{\#1}$	91.60(6)	O(1)Co(1)N(1)$^{\#1}$	92.12(6)
O(5)Co(1)N(1)$^{\#1}$	87.88(6)	N(1)$^{\#1}$Co(1)N(1)	180.00(9)
O(3)$^{\#2}$Co(2)O(3)	165.49(11)	O(3)$^{\#2}$Co(2)N(2)$^{\#1}$	97.69(7)
O(3)Co(2)N(2)$^{\#1}$	91.55(8)	N(2)$^{\#1}$Co(2)N(2)$^{\#3}$	100.82(12)
O(3)$^{\#2}$Co(2)O(4)$^{\#2}$	61.78(7)	O(3)Co(2)O(4)$^{\#2}$	107.48(7)
N(2)$^{\#1}$Co(2)O(4)$^{\#2}$	158.60(7)	N(2)$^{\#3}$Co(2)O(4)$^{\#2}$	86.55(8)
O(4)$^{\#2}$Co(2)O(4)	93.80(11)		

* Symmetry codes for compounds: (**I**) $^{\#1}$ $-x, -y+1, -z+1$; (**II**) $^{\#1}$ $x+1, -y+1/2, z+1/2$; (**III**) $^{\#1}$ $-x+1/2, -y+1/2, -z$; $^{\#2}$ $-x+1, y, -z+1/2$; $^{\#3}$ $x+1/2, -y+1/2, z+1/2$.

2.1007(16) Å) and two nitrogen atoms from two symmetry-related Bipy ligand in the axial positions (Co(1)–N(1) 2.1640(17) Å).

Each Bipy molecule bridges the adjacent Co(II) atoms to yield a straight $[Co(Bipy)]_n$ chain due to the rigid of Bipy ligand. Notably, there are eight kinds of H-bonding interactions due to the the presence of four coordinated water molecules and dissociative Cpp anion. Details of the hydrogen bonding geometry are given in Table 3. The hydrogen atoms of the coordinated water molecules and the uncoordinated carboxylic oxygen atoms are engaged in hydrogen bonding interactions with O(1*w*)–H(1*w*)···O(5), O(1*w*)–H(2*w*)···O(7), O(2*w*)–H(3*w*)···O(7), O(3*w*)–H(5*w*)···O(7), O(3*w*)–H(6*w*)···O(5), O(4*w*)–H(7*w*)···O(6), and O(4*w*)–H(8*w*)···O(8) resulting in the formation of a two-dimensional structure in the *xz* plane (Fig. 2b), and further hydrogen bonding interactions with O(2*w*)–H(4*w*)···O(6) developing the 2D layer to 3D supramolecular architecture (Fig. 2c).

Complex **III** containing Cpp anion and kinked Bds coligand generate 1D double-stranded chain, and further developing the 3D supermolecule structure in the H-bonding interaction. As revealed by single-crystal

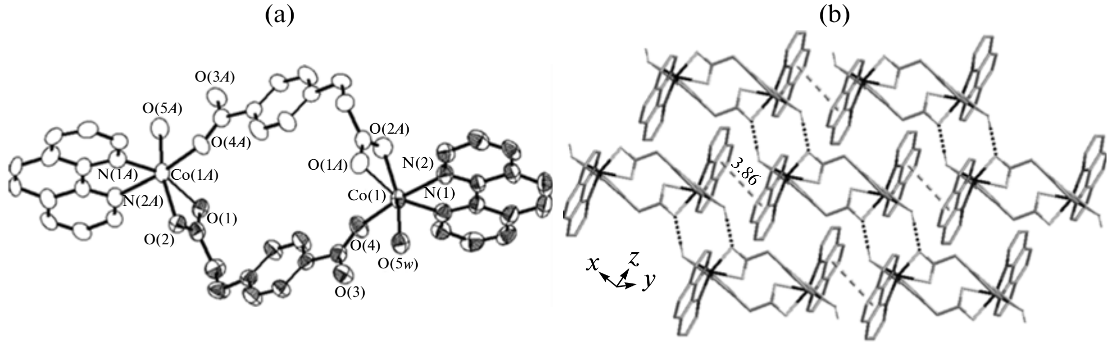

Fig. 1. ORTEP plot of the asymmetric unit showing the coordination environment of Co cation in **I** with the symmetry related part drawn in open circles. Thermal ellipsoids are given at 30% probability. Symmetry codes: (*A*) $-x$, $1 - y$, $1 - z$ (a). 2D network via π–π stacking interactions of **I** (b).

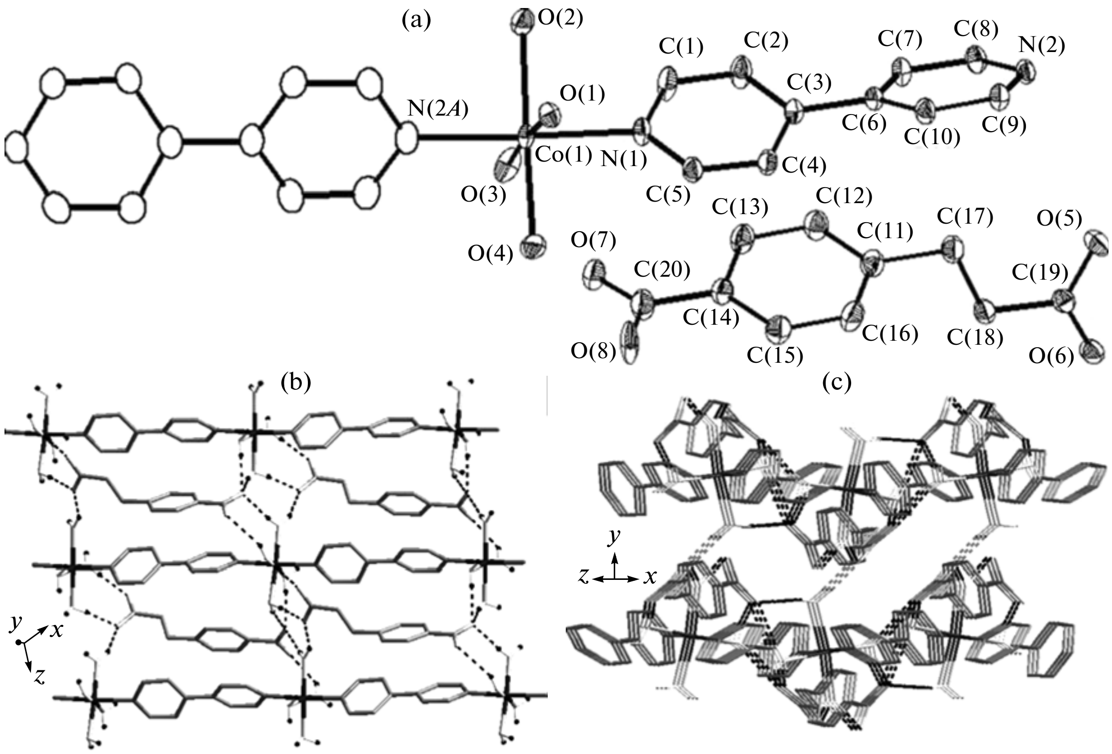

Fig. 2. ORTEP plot of the asymmetric unit showing the coordination environment of Co cation in **II** with the symmetry related part drawn in open circles. Thermal ellipsoids are given at 30% probability. Symmetry codes: (*A*) $1 + x$, $0.5 - y$, $0.5 + z$ (a). 2D network via part H-bonded interactions between coordinated water and Cpp anion (b). 3D supermolecule structure via H-bonded interactions between coordinated water and Cpp anion (c).

X-ray diffraction, the asymmetric unit of complex **III** contains two one-half Co^{2+} ion, one Cpp anion, one Bds coligand, and one ligated water molecule, as shown in Fig. 3a. Both crystallographically distinct Co atom display distorted $[CoO_4N_2]$ octahedral coordination geometry, where the Co(1) is coordinated by two carboxylate O donors of two symmetry-related Cpp anions, two coordinated water molecules, and two N donors, whereas the Co(2) is coordinated by four carboxylate O donors of two symmetry-related Cpp anions and two N-based ligands.

Extension of the structure through the combined actions of the bidentate chelating/monodentate Cpp ligand and bridging Bds coligand results in a 1D double-stranded chain that propagates along the *x* crystal direction (Fig. 3b). Adjacent double-stranded chains are subsequently conjoined into three-dimensional supermolecule structures in the H-bonding interactions (Figs. 3c, 3d). Details of the hydrogen bonding

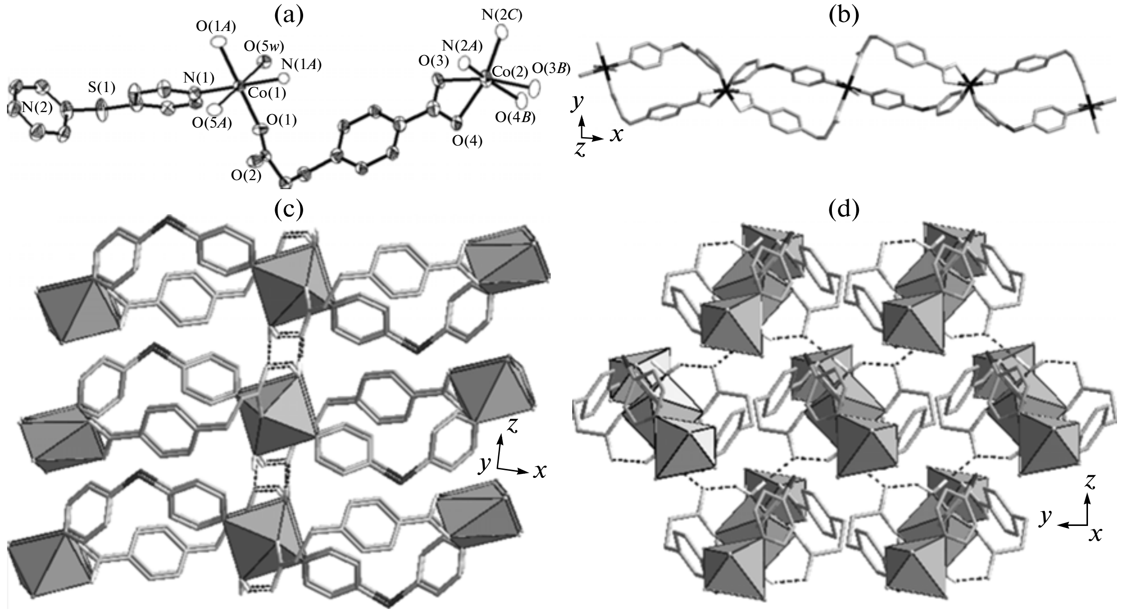

Fig. 3. ORTEP plot of the asymmetric unit showing the coordination environment of Co cation in **III** with the symmetry related part drawn in open circles. Thermal ellipsoids are given at 30% probability. Symmetry codes: (*A*) $0.5 - x, 0.5 - y, -z$; (*B*) $1 - x, y, 0.5 - z$; (*C*) $0.5 + x, 0.5 - y, 0.5 + z$ (a). 1D double-stranded chain bridged Cpp and Bds ligands (b). 3D supermolecule structure via H-bonded interactions along with the *xz* plane (c) and along with *yz* plane (d).

geometry are given in Table 4. Besides intramolecular $O(5w)-H(2w)\cdots O(2)$ hydrogen bonds, intermolecular $O(5w)-H(1w)\cdots O(2)$ interactions contribute to further extending 3D architecture.

To study the influence of additional ligands on the structure of a series of MOFs, we choose three kinds of different bridged-mode auxiliary ligands (Scheme) and find that the additional ligand characteristic has a decisive role in the formation of the structures. With adding chelate ancillary Phen ligands, as expected, the connectivity of the net becomes lower and only 0D structures were obtained, although H-bonding and $\pi-\pi$ stacking interactions allow the supramolecular 2D net formation of compound **I**. When the auxiliary ligands are able to act as bitopic linkers, for example the Bipy ligand, the net is extended to 1D chain without considering the H-bonding interaction. However, the stiffness of Bipy ligand limits the coordination impacts of the Cpp anion and cobalt metal so that the Cpp anion exists in the crystal with the dissociative state. When the Bds is chosen as bridging ancillary ligand, the net is extended to 1D double-strand chain collectively built by the Cpp anion and Bds kinked ligand. Because the Bds ligand has a kinked disposition of its terminal sulfur atoms so as to adding the flexibility, it can afford a good opportunity to enrich the structure of target complex. Therefore, the structures of three coordination architectures are strikingly sensitive to varied N-donor ancillary ligands.

The compounds **I**–**III** are further characterized by the IR spectra, which were consistent with their structures as determined by single-crystal X-ray diffraction. The broad absorption bands centered at around 3200 cm^{-1} in all case may be attributed the $\nu(O-H)$ vibrations within ligated water molecules. The characteristic bands of dicarboxylate groups are in the usual region at 1625 and 1515 cm^{-1} of complex **I** and 1606 and 1514 cm^{-1} of complex **III** for the asymmetric stretching [20] and at about 1380 cm^{-1} for the symmetric stretching, which are attributed to the co-existence of monodentate and chelating modes of the carboxylate groups [21]. Pyridine has four ring vibrations in the region of 1615–1410 cm^{-1}, which are ascribed to stretching modes of the pyridyl rings of N-based ancillary ligands. Features corresponding to pyridyl ring puckering mechanisms are evident in the region between 840 and 600 cm^{-1}. None peak of compound **I**–**III** in 1680–1700 cm^{-1} demonstrates complete deprotonation of the H_2Cpp after forming the coordination polymers.

The polycrystalline samples of compounds **I**–**III** were subjected to thermo-gravimetric analysis under flowing N_2 in order to probe the thermal stabilities of their 3D supermolecular network, as shown in Fig. 4. The TGA curve of **I** shows that the weight loss appears in the room temperature. It means that complex **I** is unstable and decomposed in the room temperature. Compared to complex **I**, complexes **II** and **III** are stable. The TGA curve of **II** shows the first weight loss of 16.7% in the region of 78–140°C, corresponding to the elimination of ligated water molecules (calcd: 15.2%). The residual solid starts to decompose at 190°C with a series of consecutive weight losses until

Table 4. Geometric parameters of hydrogen bonds for compounds **I–III***

Contact D–H···A	Distance, Å			DHA angle, deg
	D–H	H···A	D···A	
I				
O(5)–H(1*w*)···O(3)$^{\#2}$	0.85	1.78	2.602(2)	161
O(5)–H(2*w*)···O(1)	0.85	1.91	2.763(2)	176
II				
O(4)–H(8*w*)···O(8)	0.82	2.43	3.148(4)	146
O(4)–H(7*w*)···O(6)$^{\#3}$	0.82	1.91	2.729(2)	176
O(3)–H(6*w*)···O(5)$^{\#1}$	0.82	1.95	2.690(2)	150
O(3)–H(5*w*)···O(7)	0.82	1.97	2.768(2	163
O(2)–H(4*w*)···O(6)$^{\#4}$	0.84	1.77	2.599(2)	174
O(2)–H(3*w*)···O(7)$^{\#5}$	0.82	2.04	2.848(2)	170
O(1)–H(2*w*)···O(7)$^{\#5}$	0.83	1.92	2.739(2)	168
O(1)–H(1*w*)···O(5)$^{\#3}$	0.82	1.82	2.637(2)	172
III				
O(5)–H(1*w*)···O(2)$^{\#4}$	0.85	1.90	2.751(2)	177
O(5)–H(2*w*)···O(2)$^{\#1}$	0.85	1.93	2.679(2)	146

* Symmetry codes for compounds: (**I**) $^{\#2}x+1, y, z$; (**II**) $^{\#1}x+1, -y+1/2, z+1/2$; $^{\#3}x+1, y, z+1$, $^{\#4}-x+1, y-1/2, -z+3/2$, $^{\#5}x, -y+1/2, z+1/2$; (**III**) $^{\#1}-x+1/2, -y+1/2, -z$, $^{\#4}x, -y+1, z+1/2$.

540°C. The final residual species hold a weight of 26.8% of the total sample, which cannot be specifically identified and may be a mixture. So, the complex **II** obviously undergoes two-step weight loss. However, the complexes **III** displays a series of continuous weight losses from 130 to 455°C. It is difficult to determine these weight losses accurately as these processes are overlapped with the weight losses of ligated water and organic fractions. The residual solids have the weights of 26.3% of the original samples similar to complex **I**, which also seems to be a mixture.

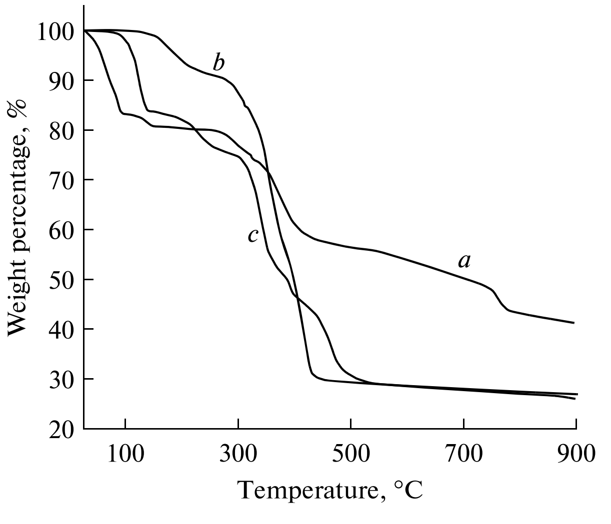

Fig. 4. TGA curves for compounds **I** (*a*), **II** (*b*), and **III** (*c*).

ACKNOWLEDGMENTS

This work was supported by the National Natural Science Foundation of China (nos. 20971064 and 21071074) and the Foundation for University Young Key Teacher by Henan Province of China (grant no. 2011 GGJS-153).

REFERENCES

1. Furukawa, H., Ko, N., Go, Y.B., et al., *Science*, 2010, vol. 329, p. 424.
2. Leshkov, Y.R., Moliner, M., and Davis, M.E., *J. Phys. Chem., C*, 2011, vol. 115, no. 4, p. 1096.
3. Millange, F., Serre, C., Guillou, N., et al., *Angew. Chem. Int. Ed.*, 2008, vol. 47, no. 22, p. 4100.
4. Xue, W., Wang, B.Y., Zhu, J., et al., *Chem. Commun.*, 2011, vol. 47, no. 37, p. 10233.
5. Liu, T., Zhang, Y.J., Wang, Z.M., et al., *J. Am. Chem. Soc.*, 2008, vol. 130, no. 32, p. 10500.

6. Yang, J., Ma, J.F., Liu, Y.Y., et al., *Cryst. Growth. Des.*, 2009, vol. 9, no. 4, p. 1894.
7. Du, M., Zhang, Z.H., Tang, L.F., et al., *Chem. Eur. J.*, 2007, vol. 13, no. 9, p. 2578.
8. Wang, Y.Q., Zhang, J.Y., Jia, Q.X., et al., *Inorg. Chem.*, 2009, vol. 48, no. 3, p. 789.
9. Huang, Y.Q., Shen, Z.L., Okamura, T., et al., *Dalton Trans.*, 2008, vol. 37, no. 2, p. 204.
10. Liu, C.S., Wang, J.J., Yan, L.F., et al., *Inorg. Chem.*, 2007, vol. 46, no. 16, p. 6299.
11. Liu, T.F., Lü, J., and Cao, R., *CrystEngComm,* 2010, vol. 12, no. 3, p. 660.
12. Bourne, S.A., Lu, J.J., Mondal, A., et al., *Angew. Chem. Int. Ed.*, 2001, vol. 40, no. 11, p. 2111.
13. Cheng, J.W., Zheng, S.T., and Yang, G.Y., *Dalton Trans.*, 2007, vol. 36, no. 36, p. 4059.
14. Chen, X.M. and Tong, M.L., *Acc. Chem. Res.*, 2007, vol. 40, no. 2, p. 162.
15. Ma, L.F., Wang, L.Y., Du, M., et al., *Inorg. Chem.*, 2010, vol. 49, no. 2, p. 365.
16. Liu, G.Z., Xin, L.Y., and Wang, L.Y., *CrystEngComm*, 2011, vol. 13, no. 8, p. 3013.
17. Liu, G.Z., Zhang, J., and Wang, L.Y., *Polyhedron*, 2011, vol. 30, no. 9, p. 1487.
18. Sheldrick, G.M., *SHELXS-97*, *Program for X-ray Crystal Structure Determination*, Göttingen (Germany): Univ. of Göttingen, 1997.
19. Sheldrick, G.M., *SHELXS-97*, *Program for X-ray Crystal Structure Refinement,* Göttingen (Germany): Univ. of Göttingen, 1997.
20. Feng, X., Tian, A.Q., Li, T.F., et al., *Russ. J. Coord. Chem.*, 2011, vol. 37, no. 11, p. 832.
21. Zhou, Y.F., Wang, R.H., Wu, B.L., et al., *J. Mol. Struct.*, 2004, vol. 697, p. 73.